

# Comparative 3D Shape Analysis of the Iwo Eleru Mandible, Nigeria

KATERINA HARVATI\*

Paleoanthropology, Institute for Archaeological Sciences and Senckenberg Center for Human Evolution and Paleoenvironment, Eberhard Karls Universität Tübingen; and, DFG Center for Advanced Studies 'Words, Bones, Genes, and Tools: Tracking Linguistic, Cultural and Biological Trajectories of the Human Past,' Eberhard Karls Universität Tübingen, Tübingen, GERMANY; [katerina.harvati@ifu.uni-tuebingen.de](mailto:katerina.harvati@ifu.uni-tuebingen.de)

CHRIS STRINGER

Centre for Human Evolution Research, The Natural History Museum, Cromwell Road, London, UNITED KINGDOM; [c.stringer@nhm.ac.uk](mailto:c.stringer@nhm.ac.uk)

CALEB ADEBAYO FOLORUNSO

Department of Archaeology and Anthropology, University of Ibadan, Ibadan, NIGERIA; [ca.folorunso@ui.edu.ng](mailto:ca.folorunso@ui.edu.ng)

\*corresponding author: Katerina Harvati; [katerina.harvati@ifu.uni-tuebingen.de](mailto:katerina.harvati@ifu.uni-tuebingen.de)

submitted: 30 May 2023; revised: 18 November 2023; accepted: 31 December 2023

Handling Editor in Chief: Karen Rosenberg

## ABSTRACT

The Iwo Eleru skeleton is the only Pleistocene human fossil currently known from western Africa. Previously, we showed morphological affinities of the Iwo Eleru cranial remains with Pleistocene archaic African specimens, consistent with former interpretations of this specimen. Those results suggested deep population substructure in Africa and a complex evolutionary process for the origin of modern humans, potentially involving hybridization between Later Stone Age modern human populations and late surviving archaic lineages. Here we conduct a geometric morphometric comparative analysis of the Iwo Eleru mandible to shed further light on the specimen's morphology and evolutionary relationships. We used twenty-five three-dimensional landmark coordinates, collected from a comparative sample comprising Pleistocene and Holocene *Homo sapiens*, as well as *Homo neanderthalensis* and Eurasian Middle Pleistocene *Homo* samples. Results show that the Iwo Eleru mandible is most consistent with the shape variation found in North African *Homo sapiens* from Epipaleolithic contexts, both in overall shape and in its large size. These findings are discussed in the temporal and geographic framework of the Iwo Eleru skeleton.

## INTRODUCTION

The Iwo Eleru<sup>1</sup> rockshelter, south-western Nigeria (Figure 1), is one of the few known Later Stone Age (LSA) sites in western Africa, and the only one yielding Pleistocene human remains. A burial, comprising a calvaria, mandible, and postcranial elements, was excavated in 1965 by Thurstan Shaw and his team in an undisturbed LSA context. An original radiocarbon date on charcoal from the burial's immediate vicinity produced a date of 11,200±200 ka (~13 ka calibrated; Shaw and Daniels 1984; see also Allsworth-Jones et al. 2010). This age estimate is in close agreement with a later direct U-series date on the skeletal remains (~11.7–16.3 ka; Harvati et al. 2011) and a more recent radiocarbon date obtained on archival charred plant material from the same layer (11,305±35 /13,207 ka cal; Cerasoni et al. 2023), placing both the skeleton and its context to the Terminal Pleistocene.

Previous studies of the cranial remains have found them to retain some archaic<sup>2</sup>-like features. Brothwell, who

reconstructed the cranium, linked it to recent West African populations but pointed out its unusual low vault and robust mandible (Brothwell and Shaw 1971). Stringer (1974) noted both modern human-like and archaic elements in his morphometric analysis of linear measurements, highlighting similarities to specimens such as Omo Kibish 2 and Saccopastore 1. More recently, Harvati et al. (2011) conducted a three-dimensional geometric morphometric analysis of the calvaria, comparing it to a large sample of recent human populations and Pleistocene fossil specimens. In that study, we found that the Iwo Eleru cranium is intermediate in shape between archaic Pleistocene humans and recent modern humans, and most similar in shape to fossils like Ngaloba and Elandsfontein. These results raised the possibility that the skeleton represents a late survival of an early *H. sapiens* population, or an admixed population with both modern human and archaic ancestry. With the advent of genomic studies showing interbreeding between modern humans and archaic 'ghost' lineages not only in Eurasia but

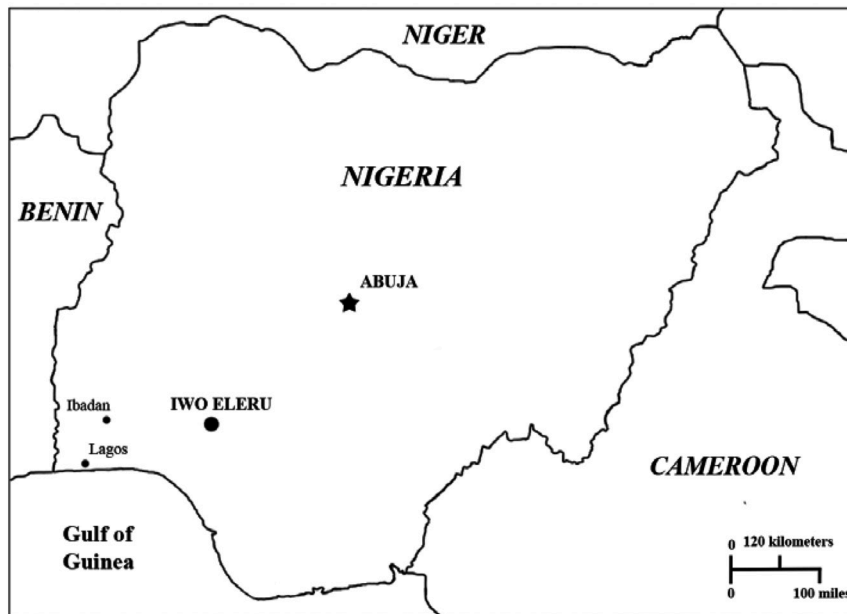


Figure 1. Map of Nigeria showing the position of the Iwo Eleru rockshelter (adapted from Harvati et al. 2011).

also in Africa (see, e.g., Harvati and Ackermann 2022; Harvati and Reyes-Centeno 2022), and specifically in western Africa (Durvasula and Sankararaman 2020; Lipson et al. 2020), the Iwo Eleru individual takes on new importance as potential fossil evidence of such past admixture events.

Here we extend our morphological investigation of the Iwo Eleru human remains by conducting a comparative three-dimensional shape analysis of its mandible, to help shed additional light on its anatomy and affinities.

#### MATERIALS AND METHODS

For the purposes of this study a high-quality cast of the Iwo Eleru mandible, housed in the Natural History Museum London, was digitized using a Microscribe (Immersion Corp. 1998) portable digitizer. The specimen is a nearly complete mandible (Figure 2), missing the condyle

and tip of the coronoid on the right side, as well as most of the teeth. Only the fourth premolars on both sides are still present, both heavily worn. The alveolar bone shows resorption. As described by Brothwell and Shaw (1971), the mandible is strongly built in both the body and rami, with a broad coronoid process and a large relatively flat condyle (left side preserved). Both anterior and posterior borders of the ascending rami slope backwards as they rise, and the gonial angles are robust and strongly everted. The mandible is broad in frontal aspect, with no clear development of a chin, while the mandibular body is relatively short but thick.

Our modern human comparative material comprised a recent southern African sample from the Dart collection (Zulu), University of the Witwatersrand, Johannesburg ( $n=20$ ) and a Holocene hunter-gatherer sample from south-



Figure 2. The Iwo Eleru mandible. Occlusal (left) and left lateral (right) views (scale = 5cm).

ern Africa, housed in the IZIKO South African Museum, Cape Town ( $n=27$ ); as well as Epipaleolithic hunter-gatherers from Afalou and Taforalt, northern Africa, housed in the Institut de Paléontologie Humaine, Paris ( $n=6$ ) (Supplementary Table 1). Our fossil comparative sample comprises three Late Pleistocene specimens from northern Africa (NAPL); fourteen Eurasian *Homo sapiens* associated with the Upper Paleolithic or correlated with this time period (EUP); the early *H. sapiens* specimens Qafzeh 9 and Skhül V (EAM); eight *Homo neanderthalensis* specimens (NEA); four Eurasian Middle Pleistocene mandibles (MPE); and, in addition to Iwo Eleru, the enigmatic Tabün 2 and Banyoles mandibles (Table 1). The latter three individuals were treated as having unknown group affiliation for the purposes of the discriminant analysis. The fossil sample included both original fossils and high-quality casts from the collections of the American Museum of Natural History, the New York University Department of Anthropology, the Smithsonian Institution, the Max Planck Institute for Evolutionary Anthropology, and the Natural History Museum. Where possible, sex samples were balanced. However, such a balance was impeded by the insecure sexing of fossil, as well as archaeological specimens included here. Given that sex is unknown for most of our fossil samples, we included samples of both sexes, as well as of indeterminate sex, in our analyses.

Three-dimensional coordinates of twenty-five mandibular landmarks were collected following the protocol published in Nicholson and Harvati (2006; see also Harvati and Lopez 2017; Harvati and Roksandic 2016; Table 2; Figure 3) representing the overall shape of the mandible. All measurements were collected by one of the authors (KH).

The raw coordinates were processed using geometric morphometric methods (for recent overviews of these methods see Mitteroecker and Schaefer 2022; Rein and Harvati 2014; Slice 2007). To maximize samples, landmarks on specimens with minimal damage were estimated during data collection, using anatomical clues from the preserved surrounding areas. For Iwo Eleru, landmarks on the alveolar bone were estimated during data collection using anatomical clues from the observed intact bone. Furthermore, bilateral landmarks missing on one side were reconstructed by superimposing the landmark configurations of specimens with missing data with their reflections and substituting the missing coordinates with their superimposed homologous counterparts on the other side ('reflected re-labeling'; Mardia et al. 2000). For Iwo Eleru this included four landmarks on the right side (right gonion, right condyle, right condyle medial, and right coronoid process). The coordinates were superimposed using Generalized Procrustes Analysis (GPA) in the PAST 4.11 software package (Hammer et al. 2001) and analyzed with principal components analysis (PCA). Iwo Eleru, Banyoles, and Tabün 2 were plotted in the PCA plots. Similarities in overall shape between Iwo Eleru and other specimens were assessed using inter-individual Procrustes distances (PD; the square root of the sum of squared distances between two superimposed landmark configurations) and shape differences

along PC axes were visualized, using the Morphologika2 2.5 software (O'Higgins and Jones 2004). Morphologika2 was also used to evaluate the relationship between centroid size and PCs 1 and 2 through a regression analysis. Similarities between Iwo Eleru and the groups analyzed were evaluated using mean PD. Because six alveolar landmarks were estimated for Iwo Eleru, all analyses were repeated using a reduced set of nineteen landmarks (M3 right and left, canine right and left, infradentale, mandibulare orale; see Table 1, see Figure 3), which were superimposed separately. Since this reduced dataset analysis will likely have reduced power, and because it is only relevant for Iwo Eleru, we only report results for this specimen. The samples were labelled as follows: *H. neanderthalensis* (NEA); Middle Pleistocene European fossils (MPE); early *H. sapiens* from Qafzeh and Skhül (EAM); Upper Paleolithic Eurasian *H. sapiens* or equivalents (EUP); North African Epipaleolithic from Afalou / Taforalt (NAEPI); North African Late Pleistocene (NAPAL); South African Holocene hunter-gatherers (SAHL); and South African recent (SARC).

## RESULTS

**Centroid size:** Similar trends were found in both the full and reduced landmark set analyses. The NEA, MPE, NAPAL, and NAEPI samples were the largest in centroid size, while SAHL were the smallest, in both analyses (Figure 4). SARC, EAM, and UPE were intermediate in size, with UPE exhibiting the greatest range of variation. Iwo Eleru and Banyoles fell in the larger end of the centroid size range, overlapping with the lower end of the MPE, NAPAL, and NAEPI range, and with the higher end of the UPE, EAM, and SARC range. Tabün 2 is even larger, overlapping with the NEA, MPE, NAPAL, and NAEPI ranges, as well as with the upper part of the UPE range.

**Principal Components Analyses:** The results of the principal components analysis (PCA) of the full dataset analysis are shown in Figure 5. PC1 (25.8% of the total variance) reflected within-taxon variation (antero-posteriorly elongate vs. short mandibles). Groups were best separated along PC 2 and 3 (13.34% and 11.45% of the variance, respectively). NEA and MPE were separated from all modern human samples along PC2, overlapping minimally with the SARC group. The archaic taxa plotted on the negative end of PC2, their convex hulls overlapping substantially. The modern human samples showed more positive PC2 scores and also overlapped extensively with each other, with the NAEPI sample being most distinctive along PC2. UPE plotted in an intermediate position, mainly showing positive PC2 values. It overlapped with NAEPI, as well as with both sub-Saharan African samples, which showed more positive PC2 scores. Both EAM specimens, as well as the three NAPAL specimens all plotted within the convex hulls of the SARC or SAHL and away from the UPE or NAEPI convex hulls. Iwo Eleru, Banyoles, and Tabün 2 were plotted into the PCA plot. Iwo Eleru fell outside the convex hulls of the two sub-Saharan samples SARC and SAHL, and closest to the NAEPI and UPE samples (see Figure 5). Banyoles also fell close to UPE and NAEPI on PC1 and 2, but also

TABLE 1. COMPOSITION OF FOSSIL COMPARATIVE SAMPLES.

Specimen	Group	Institution	Provenance	Assigned Geological Age	Reference
				(in ka)	
Qafzeh 9*	EAM	MPI-EVA	Israel	100–130	Grün et al., 2005
Skhül V*	EAM	NYU	Israel	100–130	Grün et al. 2005
Abri Pataud	EUP	MHP	France	28–26 (22 uncalibrated)	Mellars et al. 1987
Dolní Věstonice 13	EUP	IDV	Czech Rep.	ca. 31	Trinkaus and Svoboda 2006
Dolní Věstonice 14	EUP	IDV	Czech Rep.	ca. 31	Trinkaus and Svoboda 2006
Dolní Věstonice 15	EUP	IDV	Czech Rep.	ca. 31	Trinkaus and Svoboda 2006
Dolní Věstonice 16	EUP	IDV	Czech Rep.	ca. 30	Trinkaus and Svoboda 2006
Dolní Věstonice 3	EUP	IDV	Czech Rep.	undated	Trinkaus and Svoboda 2006
Grimaldi*	EUP	IPH	Italy	25 uncalibrated (ca. 29.5 cal BP)	Formicola 2004
Isturitz III	EUP	IPH	France	Upper Paleolithic	Schwartz and Tattersall 2002
Oase 1	EUP	ISC	Romania	ca. 40.5	Trinkaus 2003
Oberkassel 1*	EUP	NHM	Germany	12 uncalibrated (ca. 14.2 cal BP)	Street et al. 2006
Oberkassel 2*	EUP	NHM	Germany	12 uncalibrated (ca. 14.2 cal BP)	Street et al. 2006
Ohalo II*	EUP	IPH	Israel	19	HersHKovitz et al. 1995
Upper Cave 101*	EUP	MPI-EVA	China	ca. 35	Li et al. 2018
Upper Cave 103*	EUP	MPI-EVA	China	ca. 35	Li et al. 2018
Dar e-Soltan 5	NAPL	MMR	Morocco	75–100	Schwenninger et al. 2010; Raynal and Occhietti 2012
Nazlet Kater 2*	NAPL	NHM	Egypt	ca. 38	Crevecoeur et al. 2009
Wadi Kubbaniya*	NAPL	SIW	Egypt	ca. 20	Schild and Wendorf 2004
Amud 1*	NEA	NYU	Israel	55–60	Valladas 1999
La Ferrassie 1	NEA	MHP	France	43–45	Guérin et al. 2015
Krapina J*	NEA	AMNH	Croatia	140–120	Rink et al. 1995**
Regourdou	NEA	MHP	France	MIS 4–5	Vandermeersch and Trinkaus 1995
Shanidar 1*	NEA	AMNH	Iraq	46–50 uncalibrated	Solecki 1971
Tabūn C1	NEA	NHM	Israel	130–100	Grün and Stringer 2000; Grün et al. 2005
Zafarraya*	NEA	MPI-EVA	Spain	ca 30–46, >46	Michel et al. 2013; Wood et al. 2013

TABLE 1. COMPOSITION OF FOSSIL COMPARATIVE SAMPLES (continued).

Specimen	Group	Institution	Provenance	Assigned Geological Age	
				(in ka)	Reference
Arago 2*	MPE	AMNH	France	ca. 438	Falgueres et al. 2015
Mauer	MPE	UH	Germany	ca. 600	Wagner et al. 2010
Montmaurin	MPE	MHP	France	MIS 7	Vialet et al. 2018
Sima 5 (AT-888)*	MPE	AMNH	Spain	ca. 448	Demuro et al. 2015
Iwo Eleru*	unknown	NHM	Nigeria	ca. 11–16	Harvati et al. 2011
Banyoles*	unknown	NHM	Spain	ca. 45–66	Grün et al. 2006
Tabūn 2*	unknown	AMNH	Israel	ca. 135–170	Grün and Stringer 2000; Mercier and Valladas 2003

\*Specimens for which high quality casts were used.

\*\*Unpublished U-series analyses on mammal bones from several layers at Krapina suggest the material is at least 250,000 years old (Chris Stringer and Rainer Grün).

Group abbreviations: EAM: early *H. sapiens* from Qafzeh and Skhūl; EUP: Upper Paleolithic Eurasian *H. sapiens* or equivalents; NAPAL: North African Late Pleistocene; NEA: *H. neanderthalensis*; MPE: Middle Pleistocene European fossils. Institution abbreviations: AMNH: American Museum of Natural History, New York; IDV: Institute Dolní Věstonice; IPH: Institut de Paléontologie Humaine, Paris; ISC: Institute of Speleology, Cluj; MHP: Musée de l'Homme, Paris; MMR: Musée Maroc, Rabat; MPI-EVA: Max Plank Institute for Evolutionary Anthropology, Leipzig; NHM: Natural History Museum, London; NYU: New York University; SIW: Smithsonian Institute, Washington, D.C.; UH: University of Heidelberg.

TABLE 2. MANDIBULAR LANDMARKS USED (landmark definitions after Nicholson and Harvati 2006).\*

1. Gonion (bilateral): Point along rounded posteroinferior corner of mandible where line bisecting angle between body and ramus would hit
2. Posterior ramus (bilateral): Point at posterior margin of ramus at level of M3
3. Condyle tip (bilateral): Most superior point on mandibular condyle
4. Condylion mediale (bilateral): Most medial point on mandibular condyle
5. Root of sigmoid process (bilateral): Point where mandibular notch intersects condyle
6. Mandibular notch (bilateral): Most inferior point on mandibular notch
7. Coronion (bilateral): Most superior point on coronoid process
8. Anterior ramus (bilateral): Point at anterior margin of ramus at level of M3
9. M3 (bilateral): Point on alveolar bone just posterior to midline of third molar
10. Mental foramen (bilateral): Point in middle of mental foramen
11. Canine (bilateral): Point on alveolar margin between canine and third premolar
12. Gnathion: Most inferior midline point on symphysis
13. Infradentale: Midline point at superior tip of septum between mandibular central incisors
14. Mandibular orale: Most superior midline point on lingual side of mandible between two central incisors

\*Landmarks 9 (bilateral), 11 (bilateral), 13, and 14 were excluded in the reduced 19 landmark dataset analysis.

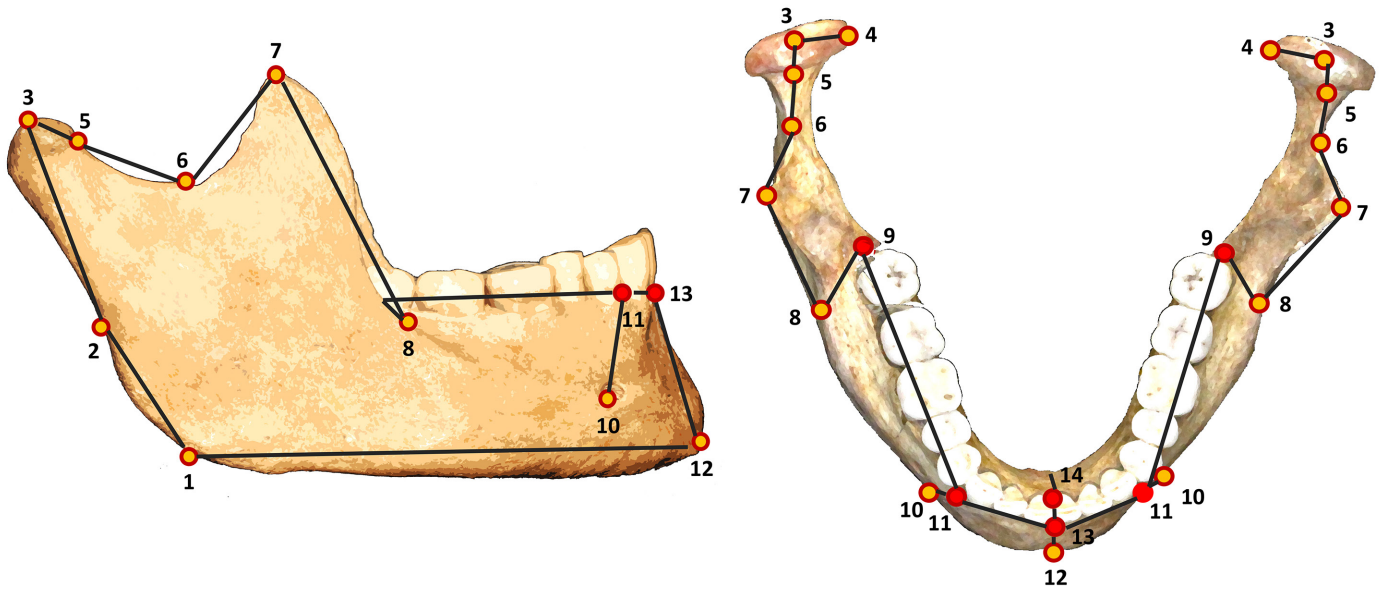


Figure 3. The 25 landmarks used in the analyses, shown as red-gold dots on a human mandible. Red dots represent landmarks that were estimated in Iwo Eleru and excluded in the reduced dataset analysis of 19 landmarks. Black lines between the dots represent the wireframe used to visualize shape changes in the Principal Components Analysis. Lateral view (left); Occlusal view (right).

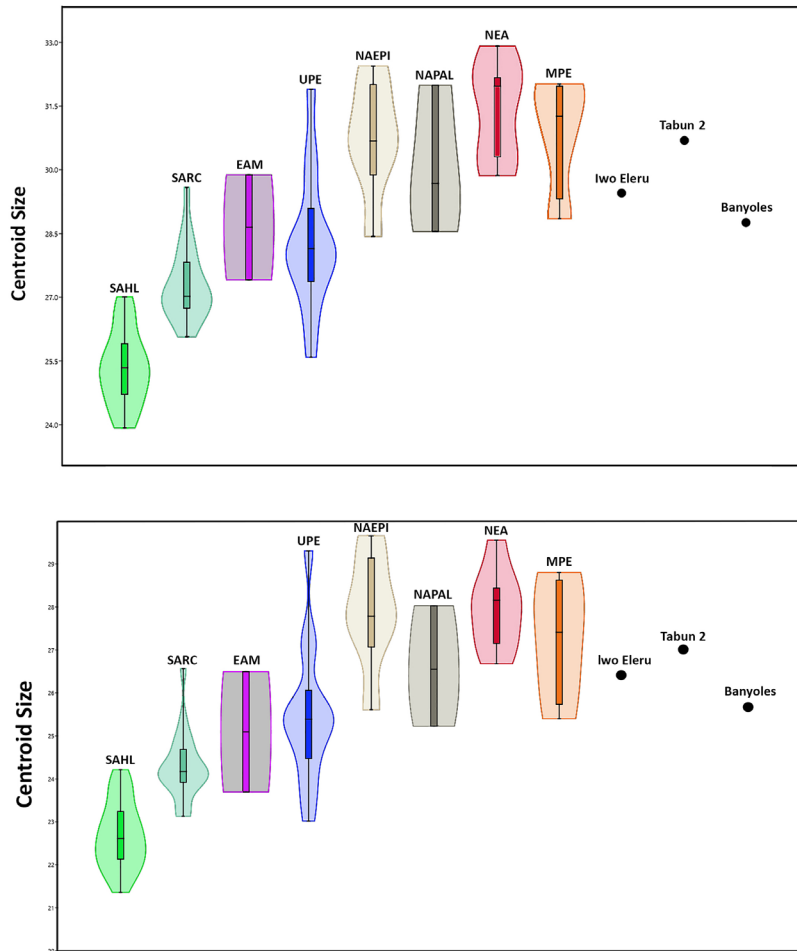


Figure 4. Centroid size by sample. 25 landmark analysis (top); reduced 19 landmark analysis (bottom). Violin plots show minimum to maximum values; superimposed box plots show median and 25%–75% quartiles.

## The Iwo Eleru Mandible • 105

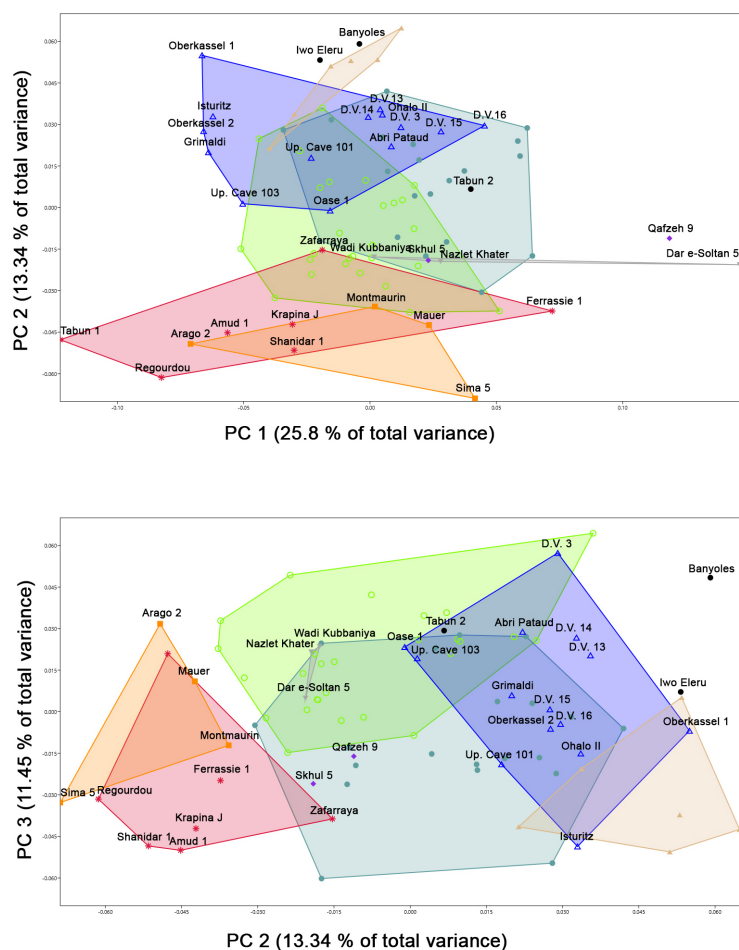


Figure 5. PC1 plotted by PC2 (top) and PC2 plotted by PC3 (bottom), 25 landmark analysis. Red stars: NEA; orange squares: MPE; green dots: SAHL; teal dots: SARC; tan dots: NAEPI; blue triangles: UPE; grey triangles: NAPAL; purple diamonds: EAM; black dots: Iwo Eleru, Banyoles, Tabūn 2. Filled in areas show the convex hulls of each of the samples.

shows a high positive PC3 value, which places it far from all convex hulls on PC2 and 3. By contrast, Tabūn 2 plotted centrally, falling within the SARC convex hull on PC1 and 2, and within both the SAHL and UPE on PC2 and 3. Neither PC1 nor PC2 were related to the size of the specimens, as measured by centroid size ( $R^2=0.003$ ,  $p=0.601$ ;  $R^2=0.011$ ,  $p=0.35$ , respectively).

Shape differences along the Principal Components 1–3 are shown in Figure 6. While PC1 and PC3 describe within-group variation (PC 1: elongated and narrow vs. wide and antero-posteriorly short; PC 3: tall and narrow vs. short and broad ramus, unequal vs. equal height of condyle and coronoid process), PC2 reflects shape differences that separate modern humans from Neanderthals and other archaic specimens. Key shape differences along this axis include a receding symphysis, more anterior placement of the third molar relative to the ramus and an asymmetric notch, with a coronoid process that is taller than the condyle characterizing modern human samples (see Figure 6), consistent with the described typical mandibular morphological differences between Neanderthals and modern humans (see, e.g., Harvati 2015).

In order to assess the influence of the inclusion of the six estimated alveolar landmarks, we repeated the analysis excluding these landmarks. Results of the PCA for the reduced dataset analysis are shown in Figure 7. Here there was more overlap between archaic and modern groups, as could be expected from a reduced landmarks analysis. NEA and MPE were only partially distinct from modern human samples on PC1, their convex hulls overlapping not only with each other, but also with UPE, SARC, and SAHL on PC1–2 (together representing 43.55% of the total variance). As with the full dataset analysis, Iwo Eleru, Banyoles, and Tabūn 2 were plotted into the PCA plot. Iwo Eleru fell within the UPE convex hull, at the border of both the NEA and NAEPI ranges.

**Procrustes Distances:** Finally, the Procrustes distances among individuals showed that Iwo Eleru was closest in overall shape to an individual from Taforalt (Taforalt H, a presumed male individual). The average Procrustes distances between Iwo Eleru (Table 3) and each of the included samples also showed closest shape similarity to the NAEPI (Afalou / Taforalt). The Banyoles mandible was closest in inter-individual Procrustes distance to a recent

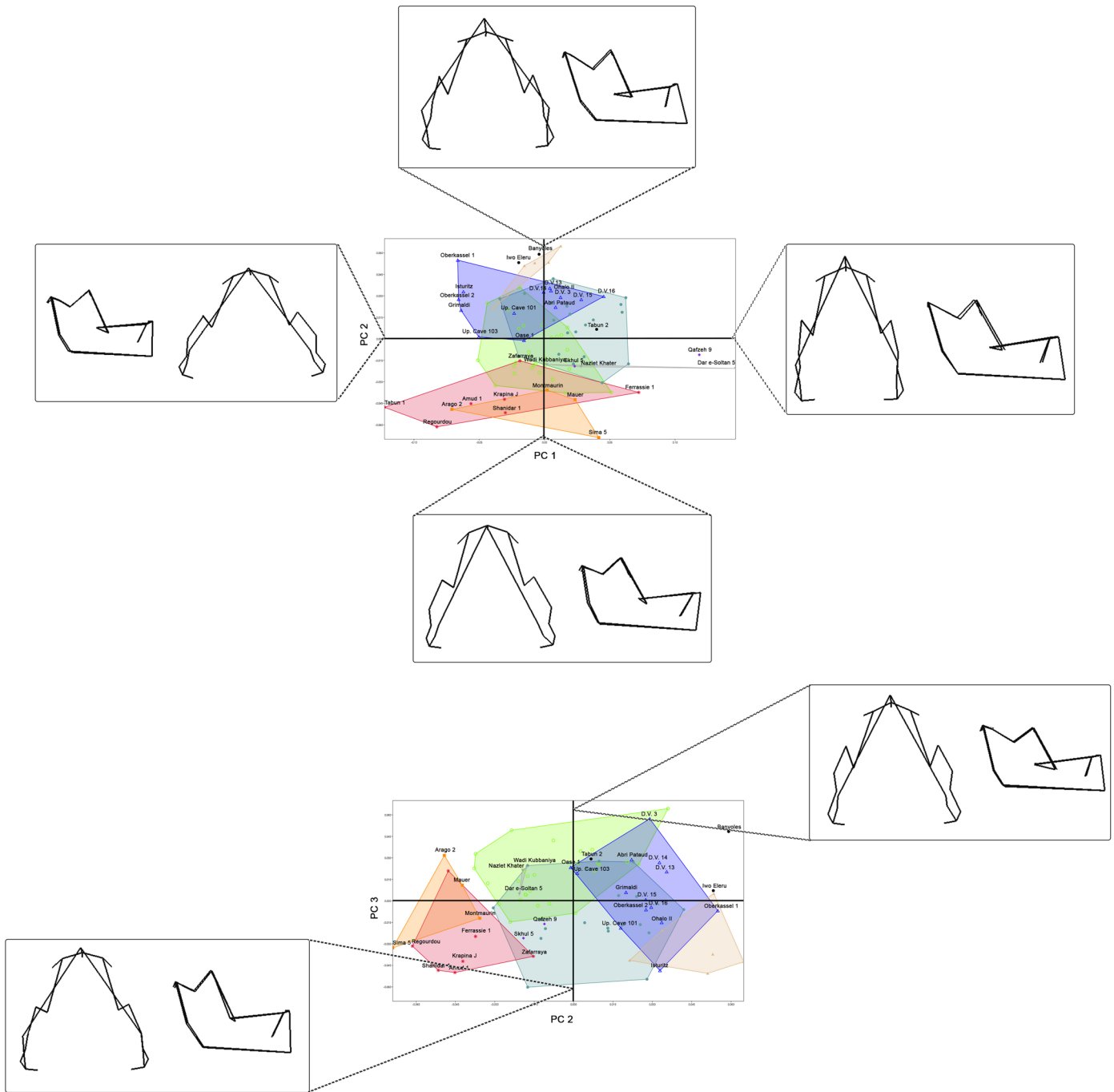


Figure 6. Shape differences along principal components 1–3, superior and lateral views. Wireframes as in Figure 3. Dashed lines indicate where on the PC axes shape was visualized.

sub-Saharan African male individual. However, it showed the smallest average distance to the UPE sample. Tabūn 2 was closest in Procrustes distance to Sima 5 and showed the lowest average distance to the MPE. The Procrustes distances were also calculated for the reduced landmarks dataset, to account for any bias introduced by the estimated alveolar landmarks on Iwo Eleru. Again, Iwo Eleru is closest in overall shape to Taforalt H, and in average Procrustes distance to the NAEPI sample (see Table 3).

## DISCUSSION AND CONCLUSIONS

Previous work on Pleistocene hominins has found that mandibular shape is largely consistent with a phylogenetic signal (Nicholson and Harvati 2006). More recently, hemimandible shape was found to broadly follow expectations for hybridization between Neanderthals and modern humans in Late Pleistocene Eurasians (Harvati and Ackermann 2022). However, other studies have indicated that, unlike other components of the skull (e.g., Harvati and

The Iwo Eleru Mandible • 107

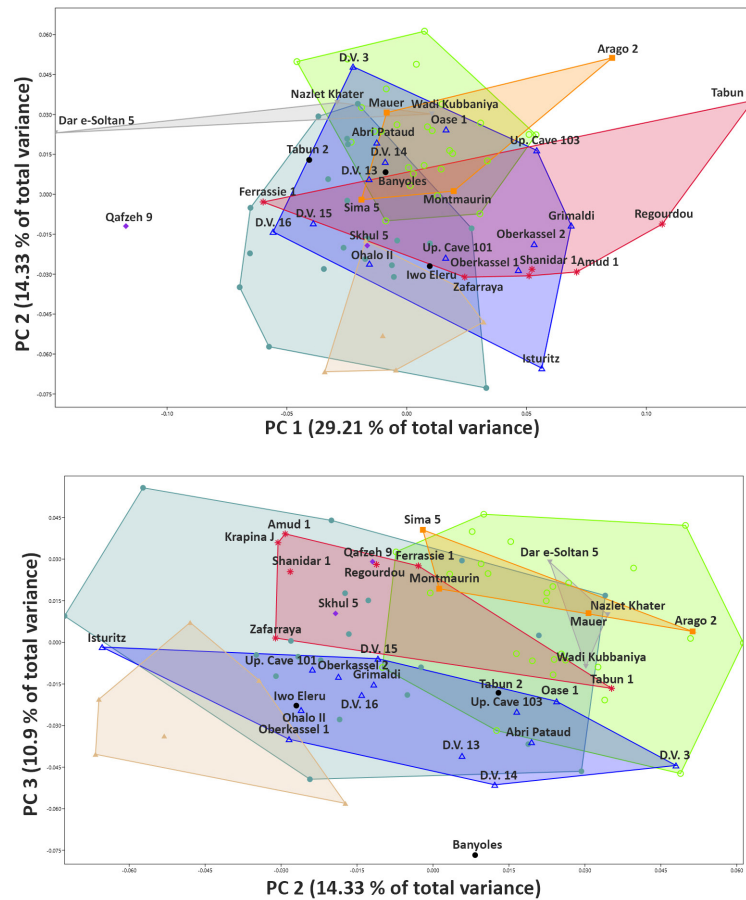


Figure 7. PC1 plotted by PC2 (top) and PC2 plotted by PC3 (bottom), 19 landmark analysis. Symbols as in Figure 5.

TABLE 3. MEANS OF THE PROCRUSTES DISTANCES BETWEEN IWO ELERU, BANYOLES, AND TABŪN 2 TO THE SAMPLES ANALYZED BASED ON THE ANALYSIS OF 25 LANDMARKS.\*

	Iwo Eleru	Banyoles	Tabūn 2	Iwo Eleru 19 landmarks
SAHL	0.1029	0.1253	0.1171	0.0940
SARC	0.0981	0.1238	0.1153	0.0898
EAM	0.1418	0.1507	0.1207	0.1269
UPE	0.1029	<b>0.1205</b>	0.1361	0.0946
NAEPI	<b>0.0898</b>	0.1278	0.1334	<b>0.0759</b>
NAPAL	0.1488	0.1527	0.1292	0.1420
NEA	0.1274	0.1561	0.1412	0.1147
MPE	0.1242	0.1422	<b>0.1114</b>	0.1046
Banyoles	0.1227	0	0.1375	0.1227
Tabūn 2	0.1354	0.1375	0	0.1168

\*For Iwo Eleru, the distances were also calculated with a reduced 19 landmark dataset. The smallest average distances are shown in bold.

Weaver 2006; Reyes-Centeno et al. 2017; Smith 2009), recent human mandibular shape variation does not correlate with neutral genetic variation (Smith 2009), suggesting that it is not a good indicator of population history. In contrast, the mandible has instead been proposed to reflect masticatory pressures and differences in subsistence strategies between hunter-gatherer populations and agriculturalists (von Cramon-Taubadel 2011; but see Katz et al. 2017, who found the influence of these factors to be relatively small compared to population history). Additionally, the mandible is known to be sexually dimorphic among modern humans. (White et al. 2011). Therefore, since multiple factors, including phylogeny and population history but also sex, behavior, and environment, are expected to influence mandibular shape and size, the analysis of the Iwo Eleru mandibular morphology must be interpreted with caution.

Our analyses suggest affinities between the Iwo Eleru mandible and the Epipaleolithic North African sample from Afalou / Taforal (NAEPI) in both its overall shape and size. This finding also persists in the reduced landmark analysis and is supported by the position of Iwo Eleru in the PCA plots as well as by the interindividual and average Procrustes distances. Its large overall size falls within the range of the North African Paleolithic and Epipaleolithic samples, as well as that of the Middle Pleistocene sample included here. These results are similar to previous findings for the early Holocene mandibular samples from Nataruk, Kenya (Mounier et al. 2018), which were also found to exhibit large size and overall shape affinities to North African Pleistocene and Epipaleolithic samples. Unlike the Nataruk specimens, however, Iwo Eleru was not found to be similar to the earlier specimens from Nazlet Khater 2, Dar e-Soltan 5, and Wadi Kubbaniya (our NAPAL sample) in our analyses. Iwo Eleru's affinities to the North African Epipaleolithic may indicate population movement across the Sahara close to the time of its life, perhaps linked to favorable climatic intervals (see also Bergman et al. 2022; Mounier et al. 2018). However, we note that our NAEPI sample is very small and likely sex biased, comprising only six individuals, five of which are presumed to be male. This hypothesis must therefore be tested further in the future.

Unlike the cranial remains of the same individual, we did not find any overall shape similarities of the Iwo Eleru mandible to earlier Pleistocene samples. This is not necessarily surprising, given the disparate influence of phylogeny and environmental factors in the mandible versus the neurocranium, the former generally considered to be affected by subsistence behavior, as well as sexual dimorphism, more than the latter (see discussion in, e.g., Nohack and Harvati 2015; Smith 2009; von Cramon-Taubadel 2011). Furthermore, if the ancestral-like shape of the Iwo Eleru neurocranium resulted from interbreeding with an archaic lineage—or with a more basal *sapiens* lineage (see, e.g., Ragsdale et al. 2023)—we would not necessarily expect to see a similar effect on the shape of the mandible: recent work has shown that different anatomical elements may preserve hybridization signals differently, even in the same individuals (Harvati and Ackermann 2022), and that any

effects on morphology likely depend on the particular archaic alleles inherited, which may be relevant for one aspect of anatomy but not another (see Gunz et al. 2019; Harvati and Ackermann 2022). The large size of Iwo Eleru could be consistent with an interbreeding scenario, since size effects, and particularly unusually large size, are among the most common consequences of hybridization (see, e.g., Harvati and Ackermann 2022). Indeed, the mandible Oase 1, the Upper Paleolithic *H. sapiens* specimen with the highest Neanderthal genetic component currently known (Fu et al. 2015), is exceptional for its large size but does not show marked shape similarities with Neanderthals (Harvati and Ackermann 2022; Harvati and Roksandic 2016). Nevertheless, size is also related to sex (White et al. 2011) in modern human mandibles, and large size may also represent the retention of an ancestral condition (see also Bergmann et al. 2021), since it also characterizes the Paleolithic and Epipaleolithic samples included here.

The Banyoles mandible was recently analyzed using 3-D geometric morphometrics using very similar landmarks and samples to ours (Keeling et al. 2022). That study found that this specimen was clearly not Neanderthal despite its geological age between  $45 \pm 4$  ka and  $66.0 \pm 7.0$  ka (Grün et al. 2006). In contrast to Keeling et al. (2022), our analysis included a more extended sample of Upper Paleolithic mandibles, as well as both Holocene and Pleistocene samples from Africa. Our results were nearly identical to those reported for the geometric morphometric analysis by Keeling et al. (2022): Banyoles clearly falls away from Neanderthals or Middle Pleistocene Europeans and aligns with modern humans. Moreover, like Keeling et al. (2022), we also found Banyoles to mainly align with the Upper Paleolithic sample in overall shape, showing the nearest average Procrustes distance to this sample, although it fell outside any sample's convex hull in our Principal Components Analysis. Interestingly, the second nearest Procrustes distance from Banyoles was to the Dolní Věstonice 13 mandible, a specimen not included in the analysis of Keeling et al. (2022). Keeling et al. (2022) concluded that the Banyoles mandible does not clearly align with *H. sapiens* due mainly to its chin morphology, which was not examined in detail here. Further study of this individual is therefore warranted to further clarify its status. Nevertheless, it adds to the increasingly recognized complexity of the European Middle and Late Pleistocene record, which suggests previously unknown early incursions of early *H. sapiens* into the continent (Harvati and Reyes-Centeno 2022; Harvati et al. 2019; Slimak et al. 2022).

Finally, the Tabūn 2 mandible plotted with modern humans in the PCA. It was found to be closest in shape to Sima 5 and to the MPE sample. These contradictory results are similar to those reported by Harvati and Lopez (2017), who found that Tabūn 2 did not show clear affinities with either Neanderthals or early modern humans, but instead tended to group with geologically older, Middle Pleistocene specimens, in their 3D shape analysis. These findings suggest that Tabūn 2 does not fit well with the samples included in the analysis, perhaps indicating that the popula-

tion that it belonged to is not represented sufficiently, or at all, in our samples.

The present analysis also differs from previous work with respect to the patterns of variation shown by Eurasian late Pleistocene modern humans compared with sub-Saharan Africans and Neanderthals. In contrast to the findings of Harvati and Ackermann (2022), here we did not find the UPE sample to be intermediate between Neanderthals and sub-Saharan Africans. Rather it mainly overlapped with Africans or was transgressive in the opposite direction. These differences in the results may be partially due to differences in the variables analyzed (complete mandibles versus hemimandibles) and in sample composition (the present analysis having much larger samples of sub-Saharan Africans). Future work should therefore seek to further investigate the potential effects of hybridization on mandibular shape using extended samples, ideally also including a greater representation of early modern and pre-modern African fossil specimens.

### ENDNOTES

<sup>1</sup>The spelling of the name of the site was changed to 'Iho Eleru' in recent publications. 'Iho' in Yoruba signifies 'a hole', while 'Iwo' in Yoruba etymology is a prefix used in names for some human habitations. Since 'Iwo Eleru' remains the name of the site as known in Nigeria, we retained the original spelling by Thurstan Shaw.

<sup>2</sup>CS prefers to use 'basal' and 'derived' in place of terms like 'archaic' and 'modern.'

### ACKNOWLEDGMENTS

We thank the NHM Collections Staff for access to the cast of the Iwo Eleru mandible and the NHM Photo Unit. We are grateful to all curators and institutions who provided permission and access to the recent, fossil, and cast samples from their collections included here, including the Institut de Paléontologie Humaine (Paris), the Musée de l'Homme (Paris), the Natural History Museum (London), the Institute at Dolní Věstonice (Dolní Věstonice), the Institute of Speleology (Cluj), the Musée Maroc (Rabat), the South African Museum IZIKO (Cape Town), the University of Heidelberg, the University of the Witwatersrand (Johannesburg), the American Museum of Natural History (New York), the New York University Department of Anthropology (New York), the Smithsonian Institution (Washington, D.C.), and the Max Planck Institute for Evolutionary Anthropology (Leipzig). All materials were studied with permission from the relevant institutions. We also thank Dr. M. Ioannidou for editorial assistance. KH is supported by the European Research Council (ERC AdG 101019659 'FIRSTSTEPS'), the Deutsche Forschungsgemeinschaft (DFG FOR 2237), and the University of Tübingen. CS is supported by Calleva Foundation (Grant Number SDV17014) and the Human Origins Research Fund. We are grateful to Aurélien Mounier and two anonymous reviewers for their helpful comments, which greatly improved this manuscript.

### DATA AVAILABILITY STATEMENT

The dataset used will be made available at the Zenodo depository upon publication.

This work is distributed under the terms of a [Creative Commons Attribution-NonCommercial 4.0 Unported License](https://creativecommons.org/licenses/by-nc/4.0/).



### REFERENCES

- Allsworth-Jones, P., Harvati, K., Stringer, C., 2010. The archaeological context of the Iwo Eleru cranium from Nigeria and preliminary results of new morphometric studies. In: Allsworth-Jones, P. (Ed.), *West African Archaeology: New Developments, New Perspectives*, British Archaeological Reports International Series 2164. Archaeopress, Oxford, pp. 29–42.
- Bergmann, I., Hublin, J.J., Ben-Ncer, A., Sbihi-Alaoui, F.Z., Gunz, P., Freidline, S.E., 2022. The relevance of late MSA mandibles on the emergence of modern morphology in Northern Africa. *Sci. Rep.* 12(1), 8841.
- Bergmann, I., Hublin, J.J., Gunz, P., Freidline, S.E., 2021. How did modern morphology evolve in the human mandible? The relationship between static adult allometry and mandibular variability in *Homo sapiens*. *J. Hum. Evol.* 157, 103026.
- Brothwell, D., Shaw, T., 1971. A late Upper Pleistocene proto-west African Negro from Nigeria. *Man (new series)* 6 (2), 221–227.
- Cerasoni, J.N., Hallett, E.Y., Orijemie, E.A., Ashastina, K., Lucas, M., Farr, L., Höhn, A., Kiahtipes, C.A., Blinkhorn, J., Roberts, P., Manica, A., 2023. Human interactions with tropical environments over the last 14,000 years at Iho Eleru, Nigeria. *iScience* 26(3), 106153.
- Crevecoeur, I., Rougier, H., Grine, F., Froment, A., 2009. Modern human cranial diversity in the late Pleistocene of Africa and Eurasia: evidence from Nazlet Khater, Pesterca cu Oase, and Hofmeyr. *Am. J. Phys. Anthropol.* 140, 347–358.
- Demuro, M., Arnold, L.J., Aranburu, A., Sala, N., Arsuaga, J.L., 2015. New bracketing luminescence ages constrain the Sima de los Huesos hominin fossils (Atapuerca, Spain) to MIS 12. *J. Hum. Evol.* 131, 76–95.
- Durvasula, A., Sankararaman, S., 2020. Recovering signals of ghost archaic introgression in African populations. *Sci. Adv.* 6, eaax5097.
- Falguères, C., Shao, Q., Han, F., Bahain, J.J., Richard, M., Perrenoud, C., Moigne, A.M., Lumley, H., 2015. New ESR and U-series dating at Caune de l'Arago, France: a key-site for European Middle Pleistocene. *Quatern. Geochronol.* 30, 547–553.
- Formicola, V., Pettitt, P.B., Del Lucchese, A., 2004. A direct AMS radiocarbon date on the Barma Grande 6 Upper Paleolithic skeleton. *Curr. Anthropol.* 45, 114–118.
- Fu, Q., Hajdinjak, M., Moldovan, O.T., Constantin, S., Mallick, S., Skoglund, P., Patterson, N., Rohland, N., Lazaridis, I., Nickel, B., Viola, B., 2015. An early modern human from Romania with a recent Neanderthal ancestor. *Nature* 524(7564), 216–219.
- Grün, R., Maroto, J., Eggins, S., Stringer, C., Robertson, S., Taylor, L., Mortimer, G., McCulloch, M., 2006. ESR and U-series analyses of enamel and dentine fragments of the Banyoles mandible. *J. Hum. Evol.* 50(3), 347–358.

- Grün, R., Stringer, C., 2000. Tabun revisited: revised ESR chronology and new ESR and U-series analyses of dental material from Tabun C1. *J. Hum. Evol.* 39, 601–612.
- Grün, R., Stringer, C., McDermott, F., Nathan, R., Porat, N., Robertson, S., Taylor, L., Mortimer, G., Eggins, S., McCulloch, M., 2005. U-series and ESR analyses of bones and teeth relating to the human burials from Skhul. *J. Hum. Evol.* 49(3), 316–334.
- Guérin, G., Frouin, M., Talamo, S., Aldeias, V., Bruxelles, L., Chiotti, L., Dibble, H.L., Goldberg, P., Hublin, J.J., Jain, M. and Lahaye, C., 2015. A multi-method luminescence dating of the Palaeolithic sequence of La Ferrassie based on new excavations adjacent to the La Ferrassie 1 and 2 skeletons. *J. Archaeol. Sci.* 58, 147–166.
- Gunz, P., Tilot, A.K., Wittfeld, K., Teumer, A., Shapland, C.Y., Van Erp, T.G., Dannemann, M., Vernot, B., Neubauer, S., Guadalupe, T., Fernandez, G., 2019. Neanderthal introgression sheds light on modern human endocranial globularity. *Curr. Biol.* 29(1), 120–127.
- Hammer, Ø., Harper, D.A.T., Ryan, P.D., 2001. PAST: Paleontological Statistics software package for education and data analysis. *Palaeontol. Electron.* 4, 1–9.
- Harvati, K., 2015. Neanderthals and their contemporaries. In: Henke, W., Tattersall, I. (Eds.), *Handbook of Paleoanthropology*, 2nd Edition. Springer, Heidelberg, pp. 2243–2279.
- Harvati, K., Ackermann, R.R., 2022. Merging morphological and genetic evidence to assess hybridization in Western Eurasian late Pleistocene hominins. *Nat. Ecol. Evol.* 6, 1573–1585.
- Harvati, K., Lopez, E., 2017. A 3-D look at the Tabūn C2 mandible. In: Hovers, E., Maron, A. (Eds.), *Festschrift for Yoel Rak. Vertebrate Paleobiology and Paleoanthropology Series*. Springer, New York, pp. 203–213.
- Harvati, K., Reyes Centeno, H., 2022. Evolution of *Homo* in the Middle and Late Pleistocene. *J. Hum. Evol.* 173, 103279.
- Harvati, K., Röding, C., Bosman, A., Karakostis, F.A., Grün, R., Stringer, C., Karkanis, P., Thompson, N.C., Koutoulidis, V., Mouloupoulos, L.A., Gorgoulis, V.G., Kouloukoussa, M., 2019. Apidima Cave fossils provide earliest evidence of *Homo sapiens* in Eurasia. *Nature* 571, 500–504.
- Harvati, K., Roksandic, M., 2016. The human fossil record from Romania: Early Upper Paleolithic mandibles and Neanderthal admixture. In: Harvati, E., Roksandic, M. (Eds.), *Paleoanthropology of the Balkans and Anatolia: Human Evolution and its Context. Vertebrate Paleobiology and Paleoanthropology Series*. Springer, Dordrecht, pp. 51–68.
- Harvati, K., Stringer, C., Grün, R., Aubert, M., Allsworth-Jones, P., Folorunso, C.A., 2011. The Later Stone Age calvaria from Iwo Eleru, Nigeria: morphology and chronology. *PLoS One* 6(9), e24024.
- Harvati, K., Weaver, T., 2006. Human cranial anatomy and the differential preservation of population history and climate signatures. *Anat. Rec.* 288A, 1225–1233.
- Hershkovitz, I., Speirs, M.S., Frayer, D., Nadel, D., Wish-Baratz, S., Arensburg, B., 1995. Ohalo II H2: a 19,000-year-old skeleton from a water-logged site at the Sea of Galilee, Israel. *Am. J. Phys. Anthropol.* 96(3), 215–234.
- Katz, D.C., Grote, M.N., Weaver, T.D., 2017. Changes in human skull morphology across the agricultural transition are consistent with softer diets in preindustrial farming groups. *Proc. Nat. Acad. Sci.* 114, 9050–9055.
- Keeling, B.A., Quam, R., Martínez, I., Arsuaga, J.L., Maroto, J., 2023. Reassessment of the human mandible from Banyoles (Girona, Spain). *J. Hum. Evol.* 174, 103291.
- Li, F., Bae, C.J., Ramsey, C.B., Chen, F., Gao, X., 2018. Redating Zhoukoudian Upper Cave, northern China and its regional significance. *J. Hum. Evol.* 121, 170–177.
- Lipson, M., Ribot, I., Mallick, S., Rohland, N., Olalde, I., Adamski, N., Broomandkoshbacht, N., Lawson, A.M., López, S., Oppenheimer, J., Stewardson, K., 2020. Ancient West African foragers in the context of African population history. *Nature* 577(7792), 665–670.
- Mardia, K.V., Bookstein, F.L., Moreton, I. J., 2000. Statistical assessment of bilateral symmetry of shapes. *Biometrika* 87, 285–300.
- Mellars, P.A., Bricker, H.M., Gowlett, J.A.J., Hedges, R.E.M., 1987. Radiocarbon accelerator dating of French Upper Paleolithic sites. *Curr. Anthropol.* 28, 128–133.
- Mercier, N., Valladas, H., 2003. Reassessment of TL age estimates of burnt flints from the Paleolithic site of Tabūn Cave, Israel. *J. Hum. Evol.*, 45, 401–409.
- Michel, V., Delanghe-Sabatier, D., Bard, E., Barroso Ruiz, C., 2013. U-series, ESR and <sup>14</sup>C studies of the fossil remains from the Mousterian levels of Zafarraya Cave (Spain): a revised chronology of Neanderthal presence. *Quat. Geochronol.* 15, 20–33.
- Mitteroecker, P., Schaefer, K., 2022. Thirty years of geometric morphometrics: achievements, challenges, and the ongoing quest for biological meaningfulness. *Am. J. Biol. Anthropol.* 178, 181–210.
- Mounier, A., Correia, M., Rivera, F., Crivellaro, F., Power, R., Jeffery, J., Wilshaw, A., Foley, R.A., Lahr, M.M., 2018. Who were the Nataruk people? Mandibular morphology among late Pleistocene and early Holocene fisher-forager populations of West Turkana (Kenya). *J. Hum. Evol.* 121, 235–253.
- Nicholson, E., Harvati, K., 2006. Quantitative analysis of human mandibular shape using 3-D geometric morphometrics. *Am. J. Phys. Anthropol.* 131, 368–383.
- Noback, M., Harvati, K., 2015. The contribution of diet to global human cranial variation. *J. Hum. Evol.* 80, 34–50.
- O’Higgins, P., Jones, N., 2004. *Morphologika*. University of York, York.
- Ragsdale, A.P., Weaver, T.D., Atkinson, E.G., Hoal, E.G., Möller, M., Henn, B.M., Gravel, S., 2023. A weakly structured stem for human origins in Africa. *Nature* 617, 755–763.
- Raynal, J.-P., Occhietti, S., 2012. Amino chronology and an earlier age for the Moroccan Aterian. In: Hublin, J.-J., McPherron, S.P. (Eds.), *Modern Origins: A North African Perspective*. Springer, Dordrecht, pp. 79–90.
- Rein, T.R., Harvati, K., 2014. Geometric morphometrics and

- virtual anthropology: advances in human evolutionary studies. *Anthropol. Anz.* 71(1–2), 41–55.
- Reyes Centeno, H., Ghirotto, S., Harvati, K., 2017. Genomic validation of the differential preservation of population history in the human cranium. *Am. J. Phys. Anthropol.* 162, 170–179.
- Rink, W.J., Schwarcz, H.P., Smith, F.H., Radovčić, J., 1995. ESR ages for Krapina hominids. *Nature* 378, 24.
- Schild, R., Wendorf, F., 2002. Palaeolithic living sites in upper and middle Egypt: a review article. *J. Field Archaeol.* 29, 447–461.
- Schwartz, J.H., Tattersall, I., 2002. *The Human Fossil Record, Terminology and Craniodental Morphology of Genus Homo (Europe)*, Vol. 1. Wiley-Liss, Hoboken, NJ.
- Schwenninger, J.L., Collcutt, S.N., Barton, N., Bouzouggar, A., Clark-Balzan, L., El Hajraoui, M.A., Nespoulet, R., Debénath, A., 2010. A new luminescence chronology for Aterian cave sites on the Atlantic coast of Morocco. In: editors (Eds.), *South-eastern Mediterranean Peoples between 130,000 and 10,000 Years Ago*. Oxbow Books, Oxford, pp.18–36.
- Shaw, T., Daniels, S.G.H., 1984. Excavations at Iwo Eleru, Ondo State, Nigeria. *West Afr. J. Arch.* 14, 1–269.
- Slice, D.E., 2007. Geometric morphometrics. *Annu. Rev. Anthropol.* 36, 261–281.
- Slimak, L., Zanolli, C., Higham, T., Frouin, M., Schwenninger, J.L., Arnold, L.J., Demuro, M., Douka, K., Mercier, N., Guérin, G., Valladas, H., 2022. Modern human incursion into Neanderthal territories 54,000 years ago at Mandrin, France. *Sci. Adv.* 8(6), eabj9496.
- Smith, H.F., 2009. Which cranial regions reflect molecular distances reliably in humans? Evidence from three-dimensional morphology. *Am. J. Hum. Biol.* 21(1), 36–47.
- Solecki, R.S., 1971. *Shanidar, the First Flower People*. Knopf, New York.
- Street, M., Terberger, T., Orschiedt, J., 2006. A critical review of the German Paleolithic hominin record. *J. Hum. Evol.* 51, 551–579.
- Stringer, C.B., 1974. A multivariate study of cranial variation in Middle and Upper Pleistocene human populations. Ph.D. Dissertation. University of Bristol.
- Trinkaus, E., Moldovan, O., Milota, Ș., Bîlgăr, A., Sarcina, L., Athreya, S., Bailey, S.E., Rodrigo, R., Mircea, G., Higham, T., Ramsey, C.B., 2003. An early modern human from the Peștera cu Oase, Romania. *Proc. Natl Acad. Sci. USA* 100, 11231–11236.
- Trinkaus, E., Svoboda, J., 2006. *Early Modern Human Evolution in Central Europe: The People of Dolní Věstonice and Pavlov*. Oxford University Press, New York.
- Valladas, H., Mercier, N., Froget, L., Hovers, E., Joron, J.L., Kimbel, W.H., Rak, Y., 1999. TL dates for the Neanderthal site of the Amud Cave, Israel. *J. Archaeol. Sci.* 26(3), 259–268.
- Vandermeersch, B., Trinkaus, E., 1995. The postcranial remains of the Régourdou 1 Neandertal: the shoulder and arm remains. *J. Hum. Evol.* 28, 439–476.
- Vialet, A., Modesto-Mata, M., Martínón-Torres, M., Martínez de Pinillos, M., Bermúdez de Castro, J.M., 2018. A reassessment of the Montmaurin-La Niche mandible (Haute Garonne, France) in the context of European Pleistocene human evolution. *PLoS One* 13(1), e0189714.
- von Cramon-Taubadel, N., 2011. Global human mandibular variation reflects differences in agricultural and hunter-gatherer subsistence strategies. *Proc. Nat. Acad. Sci.* 108(49), 19546–19551.
- Wagner, G.A., Krbetschek, M., Degering, D., Bahain, J.-J., Shao, Q., Falguères, C., Voinchet, P., Dolo, J.M., Garcia, T., Rightmire, P.G., 2010. Radiometric dating of the type-site for *Homo heidelbergensis* at Mauer, Germany. *Proc. Nat. Acad. Sci.* 107, 19726–19730.
- White, T.D., Black, M.T., Folkens, P.A., 2011. *Human Osteology*. Academic Press, San Francisco, CA.
- Wood, R.E., Barroso-Ruiz, C., Caparrós, M., Jordá Pardo, J.F., Galván Santos, B., Higham, T.F., 2013. Radiocarbon dating casts doubt on the late chronology of the Middle to Upper Palaeolithic transition in southern Iberia. *Proc. Nat. Acad. Sci.* 110(8), 2781–2786.

# Supplement 1: Comparative 3D Shape Analysis of the Iwo Eleru Mandible, Nigeria

KATERINA HARVATI\*

*Paleoanthropology, Institute for Archaeological Sciences and Senckenberg Center for Human Evolution and Paleoenvironment, Eberhard Karls Universität Tübingen; and, DFG Center for Advanced Studies 'Words, Bones, Genes, and Tools: Tracking Linguistic, Cultural and Biological Trajectories of the Human Past,' Eberhard Karls Universität Tübingen, Tübingen, GERMANY; [katerina.harvati@fu.uni-tuebingen.de](mailto:katerina.harvati@fu.uni-tuebingen.de)*

CHRIS STRINGER

*Centre for Human Evolution Research, The Natural History Museum, Cromwell Road, London, UNITED KINGDOM; [c.stringer@nhm.ac.uk](mailto:c.stringer@nhm.ac.uk)*

CALEB ADEBAYO FOLORUNSO

*Department of Archaeology and Anthropology, University of Ibadan, Ibadan, NIGERIA; [ca.folorunso@ui.edu.ng](mailto:ca.folorunso@ui.edu.ng)*

## SUPPLEMENT 1

This file includes: Supplementary Table 1.

**SUPPLEMENTARY TABLE 1. SAMPLE COMPOSITION OF THE MODERN HUMAN COMPARATIVE SAMPLES (Sex assignment—M: male, F: female, U: unknown).**

<b>Group</b>	<b>Specimen Nr.</b>	<b>Sex (M; F; U)</b>	<b>Institution</b>
SAHL	SAM-AP 27	U	South African Museum IZIKO (Cape Town)
SAHL	SAM-AP 1443	M	South African Museum IZIKO (Cape Town)
SAHL	SAM-AP 1473	U	South African Museum IZIKO (Cape Town)
SAHL	SAM-AP 1871	F	South African Museum IZIKO (Cape Town)
SAHL	SAM-AP 4188	M	South African Museum IZIKO (Cape Town)
SAHL	SAM-AP 4813	U	South African Museum IZIKO (Cape Town)
SAHL	SAM-AP 4790	U	South African Museum IZIKO (Cape Town)
SAHL	SAM-AP 4898	U	South African Museum IZIKO (Cape Town)
SAHL	SAM-AP 4899	U	South African Museum IZIKO (Cape Town)
SAHL	SAM-AP 4905	M	South African Museum IZIKO (Cape Town)
SAHL	SAM-AP 5029	U	South African Museum IZIKO (Cape Town)
SAHL	SAM-AP 4964	U	South African Museum IZIKO (Cape Town)
SAHL	SAM-AP 5034	U	South African Museum IZIKO (Cape Town)
SAHL	SAM-AP 1157	F	South African Museum IZIKO (Cape Town)
SAHL	SAM-AP 5083	U	South African Museum IZIKO (Cape Town)
SAHL	SAM-AP 5095	U	South African Museum IZIKO (Cape Town)
SAHL	SAM-AP 5050	F	South African Museum IZIKO (Cape Town)
SAHL	SAM-AP 5048	M	South African Museum IZIKO (Cape Town)
SAHL	SAM-AP 6318	M	South African Museum IZIKO (Cape Town)
SAHL	SAM-AP 6051	U	South African Museum IZIKO (Cape Town)
SAHL	SAM-AP 6074	F	South African Museum IZIKO (Cape Town)
SAHL	SAM-AP 6319	U	South African Museum IZIKO (Cape Town)
SAHL	SAM-AP 6317	U	South African Museum IZIKO (Cape Town)
SAHL	SAM-AP 6075	U	South African Museum IZIKO (Cape Town)
SAHL	SAM-AP 4840	U	South African Museum IZIKO (Cape Town)
SAHL	SAM-AP 4844	U	South African Museum IZIKO (Cape Town)
SAHL	SAM-AP 34	M	South African Museum IZIKO (Cape Town)
SARC	WITS-A1256	F	University of the Witwatersrand (Johannesburg)
SARC	WITS-A500	M	University of the Witwatersrand (Johannesburg)
SARC	WITS-A149	M	University of the Witwatersrand (Johannesburg)
SARC	WITS-A783	M	University of the Witwatersrand (Johannesburg)
SARC	WITS-A80	M	University of the Witwatersrand (Johannesburg)
SARC	WITS-A520	M	University of the Witwatersrand (Johannesburg)
SARC	WITS-A1501	F	University of the Witwatersrand (Johannesburg)
SARC	WITS-A3791	F	University of the Witwatersrand (Johannesburg)
SARC	WITS-A206	F	University of the Witwatersrand (Johannesburg)

SARC	WITS-A1451	F	University of the Witwatersrand (Johannesburg)
SARC	WITS-A584	M	University of the Witwatersrand (Johannesburg)
SARC	WITS-A541	M	University of the Witwatersrand (Johannesburg)
SARC	WITS-A1417	F	University of the Witwatersrand (Johannesburg)
SARC	WITS-A399	M	University of the Witwatersrand (Johannesburg)
SARC	WITS-A167	M	University of the Witwatersrand (Johannesburg)
SARC	WITS-A465	M	University of the Witwatersrand (Johannesburg)
SARC	WITS-A14	M	University of the Witwatersrand (Johannesburg)
SARC	WITS-A1319	F	University of the Witwatersrand (Johannesburg)
SARC	WITS-A448	F	University of the Witwatersrand (Johannesburg)
SARC	WITS-A381	F	University of the Witwatersrand (Johannesburg)
NAEPI	Afalou 27	M	Institut de Paléontologie Humaine (Paris)
NAEPI	TaforaltA	M	Institut de Paléontologie Humaine (Paris)
NAEPI	TaforaltD	M?	Institut de Paléontologie Humaine (Paris)
NAEPI	TaforaltE	F?	Institut de Paléontologie Humaine (Paris)
NAEPI	TaforaltG	M?	Institut de Paléontologie Humaine (Paris)
NAEPI	TaforaltH	M?	Institut de Paléontologie Humaine (Paris)